

Magnetization Transfer from Inhomogeneously Broadened Lines (ihMT): Application on Multiple Sclerosis (MS)

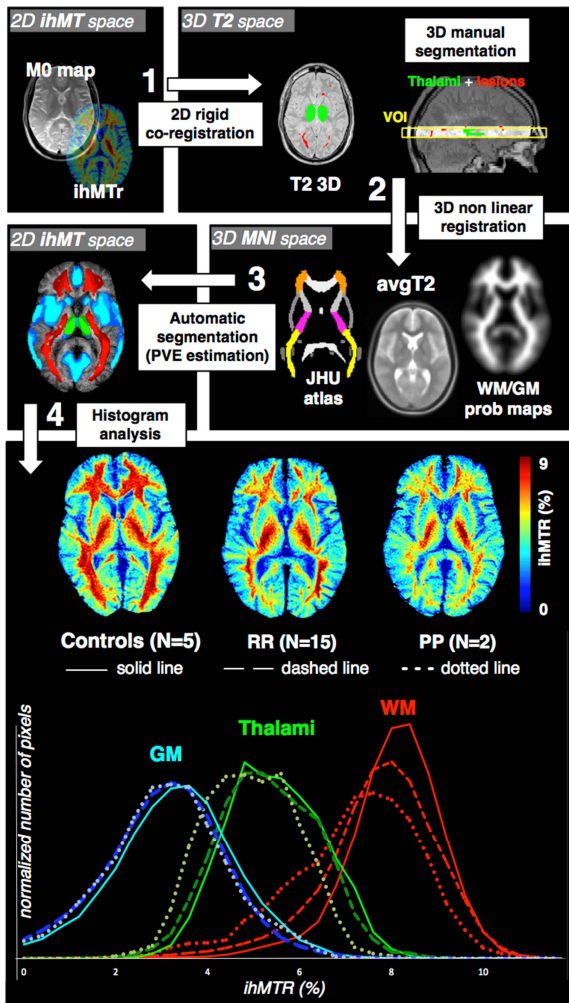
Guillaume Duhamel¹, Arnaud le Troter¹, Valentin Prevost¹, Gopal Varma², Maxime Guye¹, Jean-Philippe Ranjeva¹, Jean Pelletier³, David C. Alsop², and Olivier M. Girard¹

¹Aix Marseille University, CRMBM / CNRS UMR 7339, Marseille, France, ²Department of Radiology, BIDMC, Harvard Medical School, Boston, MA, United States,

³Pôle de Neurosciences Cliniques, Service de Neurologie, APHM, Hôpital La Timone, Marseille, France

Target audience: Scientists and clinicians interested in multiple sclerosis characterization by new myelin specific imaging techniques.

Introduction: There is a high clinical relevance of myelin-associated impairments in neurodegenerative diseases and the monitoring of myelin integrity is fundamental to understand the pathogenesis of these diseases and to assess the effect of various therapeutic scenarios in clinical research. Several techniques, including DTI, MT (qMT), and Myelin Water Fraction (MWF) have helped deepen our understanding of myelin development, damage, and repair. Unfortunately, none of these techniques is truly specific to myelin and numerous related pathologies (e.g. Multiple Sclerosis (MS)) are imperfectly characterized by current imaging methods. *Inhomogeneous Magnetization Transfer (ihMT)*^{1,2} has recently been proposed for myelin imaging. This method relies on the capacity to isolate the contribution of the inhomogeneously broadened components of the NMR spectrum. In myelin, dipolar interaction within methylene pairs in membrane lipids is thought to be responsible for inhomogeneous broadening and ihMT has demonstrated high specificity for myelinated tissues. Two key questions need however to be answered for clinics: how sensitive is ihMT for pathology? How better would ihMT do for myelin characterization compared to the current MR techniques? Preliminary clinical ihMT investigations on MS patients have been performed in order to provide insights regarding these key questions.



important in WM and accompanied with pronounced skewness of histograms (dashed/dotted lines).

Measurements performed in WM substructures indicated significant ihMTR values decrease in FWM and OWM, for both PP and RR patients compared to controls (Table 1). No change in ihMTR was observed in IC. All combined, these results clearly indicated that the ihMT technique demonstrates sensitivity to different characteristics of the pathology in MS disease. Of interest, all the significant variations observed in patients for ihMTR were more pronounced than that of classical MTR (table 1, e.g. in OWM for PP patients, MTR decreased from -8.5% and ihMTR from -21.3%, compared to controls). This suggested that, additionally to better specificity, ihMT also provided higher sensitivity than classical MT for MS characterization.

Conclusion: This preliminary clinical study investigated sensitivity of ihMT for MS disease for 2 different types of patients. Significant decrease of ihMTR values was observed in different NAWM substructures for patients. Compared to classical MT, ihMT also demonstrated higher sensitivity for pathology, as illustrated by higher ihMTR variations than MTR variations between patients and controls. These results complement prior preliminary observations⁴ and represent great promise regarding the capacity of ihMT in providing better characterization of MS. Further experiments on larger groups and with whole brain coverage would be however required.

References: ¹ Varma *et al*, Magn Reson Med (2014), ² Girard *et al*, Magn Reson Med (2014), ³ Mori *et al*, (2005), ⁴ Varma *et al*, Proc. ISMRM (2014) #p2071.

Methods: MRI. MS patients (RR, n=15, EDSS<2, 40±8y/o; PP, n=2, EDSS>2, 44±4y/o) and 5 sex/age-matched control subjects were scanned at 1.5T (Avanto MRI, Siemens, Erlangen, Germany) using anatomic imaging (axial T_{2w} (MTX 256x256, 44 slices, ST=3mm, FOV=240mm, TR/TE=2600/14ms) for lesion segmentation and image registration/segmentation) and ihMT imaging realized with a pulsed saturation preparation module² combined with a 2D HASTE readout (FOV=220mm, MTX 192x192, mid-ventricle single axial 9mm-slice, TR/TE=3s/21ms). IhMT contrast was derived from subtraction of MT images obtained with simultaneous saturation at positive and negative frequency offsets from those obtained with single frequency saturation at the same total power. Offset frequency was set to $|\Delta f| = 7\text{kHz}$ and the saturation parameters were: train of Hann-shaped pulses (length pw=0.5ms) repeated every $\Delta t=1\text{ms}$ for a total saturation time of $\tau=700\text{ms}$. Energy of saturation was $E_{\text{tr}}=B_{1\text{rms}} \times \tau = 35\mu\text{T}^2\cdot\text{s}$. MT datasets were averaged 20 times. IhMT and classical MT ratios were calculated as $\text{ihMTR} = \text{ihMTR}/S_0$ and $\text{MTR} = 1 - \text{MT} (+\Delta f)/S_0$, where S_0 is the signal measured with RF saturation power set to zero.

Semi-automatic image processing (Fig 1): **step 1.** Single slice ihMT images were co-registered on the 3D T_{2w} volume using *flirt* algorithm of FSL. This registration allowed estimating a volume of interest (VOI) in the 3D T_{2w} space, precisely corresponding to the ihMT single larger slice. Manual segmentation of thalamus and lesions was performed in the T_{2w} images contained in the VOI. **step 2.** Non-linear registration of the 3D T_{2w} volume on the average T₂ template of MNI (SPM-toolbox) using ANTS library (PR, 50 iterations). **step 3.** Resulting global WM/GM probabilistic maps for each slice contained in the VOI were cleared of lesions, then summed and finally used to automatically obtain a probabilistic global normal appearing (NA) WM/GM segmentation in the 2D ihMT space (with light colors corresponded to probability of 100%). Additionally, NAWM substructures including frontal WM (FWM), internal capsule (IC) and occipital WM (OWM) were segmented using labeled tracts JHU atlas³. **step 4.** Quantitative analysis were performed in global 100%-probabilistic masks of NA WM, GM and thalamus as well as in FWM, IC and occipital WM (OWM).

Results & Discussion: Characteristic ihMTR maps for controls, RR and PP patients are shown on figure 1. High specificity of ihMT for myelinated structures is clearly evidenced. RR (middle) and PP (right) patients showed respectively moderate and pronounced decrease of ihMTR values, especially in WM, compared to that of controls (left). This was confirmed by quantitative measurements.

Histograms of values in normal appearing WM/GM/thalamus areas, demonstrated global decrease for both PP and RR patients (dashed/dotted lines) compared to controls (plain lines). The decrease was more

	Controls (n=5)	RR (n=15) %var. w/r Controls	PP (n=2) %var. w/r Controls
MTR (%)			
FWM	49.2±0.4	47.3±1.6 / -4.00%*	47.1±2.6 / -4.55%*
IC	45.6±0.6	45.7±0.7 / +0.19%	46.1±0.4 / +1.11%
OWM	48.1±0.2	45.0±1.7 / -6.72%*	44.3±2.8 / -8.50%*
ihMTR (%)			
FWM	8.5±0.2	8.0±0.4 / -5.91% *	7.5±1.0 / -12.44% *
IC	9.3±0.2	9.4±0.3 / +0.79%	9.0±0.03 / -4.18%
OWM	9.1±0.1	8.3±0.6 / -10.07% *	7.5±1.3 / -21.27% *

Table 1: MTR and ihMTR in controls and patients. *: $p < 0.01$